Coarse particle ($PM_{10-2.5}$) source profiles for emissions from domestic cooking and industrial process in Central India

Check for updates

Shahina Bano [a], Shamsh Pervez [a,*], Judith C. Chow [e,f], Jeevan Lal Matawle [a,b], John G. Watson [e,f], Rakesh Kumar Sahu [a], Anjali Srivastava [c], Suresh Tiwari [d], Yasmeen Fatima Pervez [g], Manas Kanti Deb [a]

[a] School of Studies in Chemistry, Pt. Ravishankar Shukla University, Raipur 492010, Chhattisgarh, India
[b] Directorate of Geology and Mining, Chhattisgarh, Regional Laboratory, Jagdalpur 494001, Chhattisgarh, India
[c] National Environmental Engineering Research Institute, Nehru Marg, Nagpur 440020, Maharashtra, India
[d] Indian Institute of Tropical and Meteorology, New Delhi 110060, India
[e] Division of Atmospheric Sciences, Desert Research Institute, Reno, NV 89512, USA
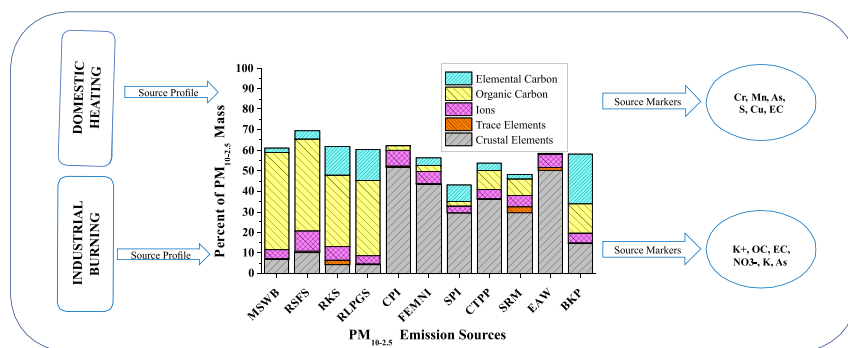[f] Institute of Earth and Environment, Chinese Academy of Science, Xian, China
[g] Department of Engineering Chemistry, CSIT, Kolihapuri, Durg, Chhattisgarh 491010, India

HIGHLIGHTS

- Carbon fractions were most abundant in household fuel and municipal solid waste combustion emissions.
- Ca was abundant in steel-rolling mill and cement production emissions, with abundant Fe in ferro-manganese and electric arc-welding process.
- Elements were more enriched in $PM_{2.5}$ than in $PM_{10-2.5}$ due to higher temperature industrial processes.

GRAPHICAL ABSTRACT

ARTICLE INFO

ABSTRACT

To develop coarse particle ($PM_{10-2.5}$, 2.5 to 10 μm) chemical source profiles, real-world source sampling from four domestic cooking and seven industrial processing facilities were carried out in "Raipur-Bhilai" of Central India. Collected samples were analysed for 32 chemical species including 21 elements (Al, As, Ca, Cd, Co, Cr, Cu, Fe, Hg, K, Mg, Mn, Mo, Na, Ni, Pb, S, Sb, Se, V, and Zn) by atomic absorption spectrophotometry (AAS), 8 water-soluble ions (Na^+, K^+, Mg^{2+}, Ca^{2+}, Cl^-, F^-, NO_3^-, and SO_4^{2-}) by ion chromatography, ammonium (NH_4^+) by spectrophotometry, and carbonaceous fractions (OC and EC) by thermal/optical transmittance. The carbonaceous fractions were most abundant fraction in household fuel and municipal solid waste combustion emissions while elemental species were more abundant in industrial emissions. Most of the elemental species were enriched in $PM_{2.5}$ (<2.5 μm) size fraction as compared to the $PM_{10-2.5}$ fraction. Abundant Ca (13–28%) was found in steel-rolling mill (SRM) and cement production industry (CPI) emissions, with abundant Fe (14–32%) in ferro-manganese (FEMNI), steel production industry (SPI), and electric-arc welding emissions. High coefficients of divergence (COD) values (0.46 to 0.88) among the profiles indicate their differences. These region-specific source profiles are more relevant to source apportionment studies in India than profiles measured elsewhere.

© 2018 Elsevier B.V. All rights reserved.

* Corresponding author.
E-mail address: shamshpervez@gmail.com (S. Pervez).

1. Introduction

The Chemical Mass Balance (CMB) receptor model with its effective variance and positive matrix factorization (PMF) solution is applicable to particulate matter (PM) and volatile organic compounds (VOCs) (Gupta et al., 2007; Samara et al., 2003; Watson et al., 2002). Source apportionment of PM from various pollution sources and the fractional mass abundances of chemical species, i.e. source profiles (Watson et al., 2001), are needed for these CMB solutions (Friedlander, 1973). Average chemical abundances in a profile are accompanied by standard deviations of repeated samples that represents the uncertainties of the averages. (Chow et al., 2003, 2004; Ho et al., 2003; Tsai et al., 2007; Watson et al., 1994, 2001). Several source profiles have been reported and assembled (Aldabe et al., 2011; Chow et al., 2004; Ning et al., 1996; Watson et al., 2001). The SPECIATE (U.S. EPA, 2013), SPECIEUROPE (Pernigotti et al., 2016), and China Source Profile Shared Service (CSPSS) (Liu et al., 2017) databases contain a large number of these profiles.

These source profiles, having diversity in geographical locations, fuel types, combustion and emission control technologies and time periods have been applied for source apportionment studies to identify and quantify PM source contributions (Watson and Chow, 2001; Yatkin and Bayram, 2008).

In developing nations, most source apportionment studies have been carried out with existing USA/Europe source profiles (Chelani et al., 2008; Gokhale et al., 2008; Gupta et al., 2007; Srivastava et al., 2009), resulting in higher uncertainties in source contribution estimates. In India, limited $PM_{2.5}$ and/or PM_{10} (particles with aerodynamic diameter <2.5 and 10 micrometers [μm], respectively), source profiles have been reported without specific $PM_{10-2.5}$ fractions (2.5 to 10 μm) (Matawle et al., 2014, 2015; Patil et al., 2013; Samiksha et al., 2017). Inhalation of $PM_{10-2.5}$ can be a cause of respiratory ailments (e.g., asthma and bronchitis) in India (Rumana et al., 2014; WHO, 2014).

This study reports $PM_{10-2.5}$ source profiles for a variety of domestic cooking and industrial process facilities in an urban-industrial environment of Central India. Reconstructed mass using measured species, coefficients of divergence (CODs), enrichment factors (EFs), and characteristic markers are examined to evaluate the similarities and differences among the profiles.

2. Methodology

2.1. Sampling site and instrumentation

Raipur-Bhilai, an industrial city of Central India (21°14′22.7″N, 81°38.1″E and 21°11′0″N, 81°23′6″E), has a population of 1.6 million (Census, 2011). The main industries (>90% of total) include coal-fired steel processing, power generation, and cement production. Around 60 and 89% of urban and rural households use solid fuels for cooking practices, respectively (Census, 2011). Emissions from domestic heating activities and municipal solid waste (MSW) burning are also important. Matawle et al. (2014) showed that 1200 tons of MSW per day is generated in Raipur-Bhilai, and approximately 65% of total MSW is disposed of by open burning.

Table 1 documents the source types, activity, types of combustion material, and sampling methods for the 11 sources included in this study. Detailed source selection, combustion processes, and sampling methods have been documented by Matawle et al. (2014, 2015). Two sampling methods were used: (1) in-plume sampling for residential fuel combustion; and (2) chamber resuspension sampling for residues (i.e. fly ash) collected in the bag-filters, (Chow et al., 2004; Chakrabarty et al., 2013; Dewangan et al., 2013; Matawle et al., 2014, 2015; Tiwari et al., 2013). Source tests were conducted with collocated PM_{10} and $PM_{2.5}$ Minivol air samplers (Airmetrics Model, Ver. 4.2) operating at a flow rate of 5 L/min. Samples were collected on quartz-fiber filters (47 mm diameter, Whatman Catalog No. 1851-047). Five sets of parallel samples were acquired from each emission source for a total of 55 samples. Mass and chemical components of $PM_{10-2.5}$ were obtained by subtracting the corresponding $PM_{2.5}$ values from PM_{10}.

Each filter was weighed before and after sampling using a single pan top loading digital balance (Denver, Model TB-2150) with a precision of ± 10 μg (Watson et al., 2017). Each sample was sectioned into four equivalent portions to analyze for 21 chemical species (Al, As, Ca, Cd, Co, Cr, Cu, Fe, Hg, K, Mg, Mn, Mo, Na, Ni, Pb, S, Sb, Se, V, and Zn) by atomic absorption spectrophotometry (AAS) (Watson et al., 2016), 8 ions (Na$^+$, K$^+$, Mg^{2+}, Ca^{2+}, Cl$^-$, F$^-$, NO$_3^-$, and SO$_4^{2-}$) by ion chromatography (Chow and Watson, 2017); ammonium (NH$_4^+$) by spectrophotometry; and carbon fractions (OC and EC) by thermal/optical transmittance carbon analyzer (Matawle et al., 2014, 2015).

Table 1
Description of eleven domestic cooking and industrial combustion sources for the study.

S.N.	Profile ID	Source type	Activity	Types of combustion material	Sampling method
Municipal solid waste combustion					
1.	MSWB	Municipal solid waste combustion	~5 major dumping zone including ~200 minor burning locations	Synthetic and natural biomaterials in a 1:8 ratio	In-plume sampling
Household fuel combustion sources					
2.	RSFS	Residential solid fuel stoves	~45% households	Conventional mixture of Coal, wood, dung with ratio in 2:1:1	In-plume sampling
3.	RKS	Residential kerosene stoves	~30% households	Kerosene	In-plume sampling
4.	RLPGS	Residential LPG stoves	~25% households	Liquid petroleum gas	In-plume sampling
Mineral-based coal-fired industries					
5.	CPI	Cement production industry	>9 major and >12 minor units	Limestone, gypsum, steel slag	Chamber re-suspension of bag-filter dust
6.	FEMNI	Ferro-manganese industry	>90 major and minor units	Iron ore, coal, dolomite, manganese ore	Chamber re-suspension of bag-filter dust
7.	SPI	Steel production industry	>130 major and minor units	Iron ore, coal, dolomite	Chamber re-suspension of bag-filter dust
8.	CTPP	Coal based thermal power plant	>50 major and minor units	Coal	Chamber re-suspension of bag-filter dust
9.	SRM	Steel rolling mills	>150 major and minor units	Scrap cuttings, steel ingots, coal	Chamber re-suspension of bag-filter dust
10.	BKP	Brick kiln process	>300 major and minor furnaces	Brick clay, coal, wood	In-plume
Workshops					
11.	EAW	Electric arc-welding	>1200 major and minor units	Iron, welding material	In-plume sampling

2.2. Quality assurance and quality control (QA and QC)

Each filter was weighed three times before and after sampling and an average of the three readings was used. After weighing, samples were individually placed in filter cassettes and packaged in an airtight polyethylene zip lock bag for refrigerated storage (<4 °C). Solutions applied to chemical analyses were prepared in deionised-double distilled water (DDW). Glassware and filter assemblies were acid washed and oven dried to minimize potential contamination.

For elemental analysis, the AAS was calibrated using a set of five standards for individual species. Linear regression calibration curves were accepted when correlation coefficient (R^2) > 0.95. Background levels were assessed with laboratory filter blanks and field blanks. Limits of detection (LOD) and species concentrations of laboratory and field blanks are summarized in Supplemental Table S1. As part of quality control (QC), one standard was analysed for every ten samples to assure the recovery range of 80%–120%. Each sample was analysed three times to ensure precisions are within ±10%.

3. Results

3.1. PM$_{10-2.5}$ chemical source profiles

The source profiles in Tables 2 and 3 consist of fractional abundances of measured chemical species and associated uncertainties (Watson et al., 2001). The sum of measured species accounted for 59–64% and 41–55% of measured PM$_{10-2.5}$ mass for domestic cooking and industrial combustion sources, respectively. The unaccounted mass may be attributed to unmeasured elements (Si and Ti), metal oxides, and water content (Ho et al., 2003; Watson et al., 2012). Carbonaceous aerosol (i.e.

Total Carbon, TC = OC + EC) accounts for ~49–51% and ~0.3–38% of PM$_{10-2.5}$ mass from domestic cooking and industrial combustion sources, respectively. Large variations in OC/EC ratios were found. With the exception of ferro-manganese (FEMNI), steel production (SPI), and brick kiln (BKP), all other industrial combustion sources, reported OC/EC ratio > 2, consistent with incomplete combustion processes (Chakrabarty et al., 2013). Combustions associated with household solid fuels (RSFS), municipal solid waste management (MSWB), electric arc-welding (EAW), and cement processing (CPI) showed the highest OC/EC ratios (11–32).

3.2. Municipal solid waste combustion (MSWB)

Open burning of solid waste is a major contributor to air pollution in India (Patil et al., 2013). TC was found to be the most abundant species and accounted for ~50% of measured PM$_{10-2.5}$ mass, with a OC/EC ratio of 19.4 and a K$^+$/K ratio of 0.69, consistent with past studies for vegetative and biomass burning (Chow et al., 2004; Watson et al., 2001, 1994).

3.3. Residential cook stoves

Residential cooking consists of three types of fuel/fuel mixtures, i.e. liquefied petroleum gas (LPG), kerosene, and solid fuel (3:1:1 ratio of coal, wood, and dung cakes) (Matawle et al., 2014). The OC/EC ratio of 11.1 for residential solid fuel stoves (RSFS) is fourfold higher than ratios for kerosene (RKS) and LPG (RLPGS) stoves. The K$^+$/K ratios (0.57–0.93) and NH$_4^+$ abundances (0.05–1.9%) are comparable to past studies (Chow et al., 2004; Kong et al., 2011; Watson et al., 1994, 2001), but they are higher than those found for the geological materials and industrial sources. Among the three household fuel types, the abundance of

Table 2
Composite PM$_{10-2.5}$ source profiles (weight percent by mass) of emissions from domestic cooking and municipal waste combustion.

Species	Source type[a]			
	RSFS	RKS	RLPGS	MSWB
Al	0.09380 ± 0.46783	2.87150 ± 2.65026	1.66120 ± 6.27956	0.08440 ± 0.25332
As	0.01531 ± 0.00940	0.00270 ± 0.00338	0.00004 ± 0.00001	0.00065 ± 0.00018
Ca	3.20051 ± 3.00512	0.14820 ± 0.78671	0.16490 ± 1.14910	1.85110 ± 1.20112
Cd	0.00003 ± 0.00011	0.00020 ± 0.00021	0.00090 ± 0.00370	0.00384 ± 0.00361
Co	0.00735 ± 0.00616	0.00040 ± 0.00068	0.00034 ± 0.00029	0.00045 ± 0.00064
Cr	0.53218 ± 0.30289	0.00903 ± 0.00710	0.02659 ± 0.03430	0.00542 ± 0.00210
Cu	0.03506 ± 0.02856	0.00169 ± 0.00481	0.00288 ± 0.00249	0.05662 ± 0.08120
Fe	0.46290 ± 0.20213	0.25120 ± 0.30262	0.05880 ± 0.06247	0.93880 ± 0.66407
Hg	0.00083 ± 0.00171	0.01337 ± 0.00865	0.00228 ± 0.00568	0.00225 ± 0.00157
K	4.14007 ± 2.00650	0.89479 ± 0.59512	0.13590 ± 0.13002	1.44246 ± 1.61424
Mg	0.29380 ± 0.27696	0.00180 ± 0.00678	0.00630 ± 0.00586	0.11790 ± 0.10612
Mn	0.01706 ± 0.01476	0.00162 ± 0.00249	0.02288 ± 0.05277	0.03678 ± 0.03150
Mo	0.00119 ± 0.00184	0.00394 ± 0.00470	0.00980 ± 0.00828	0.00208 ± 0.00136
Na	1.74690 ± 1.93060	0.14550 ± 0.36473	2.27090 ± 1.96588	2.34840 ± 1.48422
Ni	0.01274 ± 0.01250	0.13437 ± 0.14245	0.00774 ± 0.00576	0.01113 ± 0.00837
Pb	0.00001 ± 0.00002	0.33800 ± 0.17242	0.00114 ± 0.00088	0.00108 ± 0.00084
S	0.08432 ± 0.25874	0.71306 ± 1.64290	0.00126 ± 0.00049	0.00915 ± 0.19564
Sb	0.00014 ± 0.00004	0.00106 ± 0.00045	0.00120 ± 0.00022	0.00013 ± 0.00002
Se	0.00187 ± 0.00064	0.00125 ± 0.00014	0.00211 ± 0.00033	0.00715 ± 0.00177
V	0.00243 ± 0.00168	0.01555 ± 0.00527	0.00432 ± 0.00704	0.00624 ± 0.00520
Zn	0.12114 ± 0.10693	0.91267 ± 0.76408	0.03489 ± 0.03937	0.23415 ± 0.12059
F$^-$	0.06312 ± 0.04631	0.00020 ± 0.00008	0.00010 ± 0.00008	0.02802 ± 0.01280
Cl$^-$	1.68122 ± 0.53332	0.76670 ± 0.98712	0.52518 ± 0.36092	0.38138 ± 0.20016
NO$_3^-$	2.19717 ± 3.76373	1.01461 ± 0.77250	0.57716 ± 0.50241	0.21003 ± 0.08010
SO$_4^{2-}$	1.15451 ± 1.11019	2.00311 ± 1.19441	1.18518 ± 0.50140	0.46468 ± 0.16003
Na$^+$	0.64350 ± 0.88220	0.08840 ± 0.08679	1.00313 ± 1.33179	0.85198 ± 0.67400
NH$_4^+$	0.05061 ± 0.01236	1.93514 ± 0.25553	0.95427 ± 0.49266	0.75221 ± 0.16220
K$^+$	2.69008 ± 0.37050	0.51352 ± 0.10174	0.12599 ± 0.01418	0.98949 ± 0.11300
Ca^{2+}	1.30150 ± 0.85100	0.09991 ± 0.12306	0.02980 ± 0.01982	0.56364 ± 0.64120
Mg^{2+}	0.16149 ± 0.18040	0.00147 ± 0.00152	0.00532 ± 0.00434	0.06602 ± 0.04120
OC	44.77570 ± 6.13628	35.08212 ± 3.52635	36.41815 ± 1.70268	47.28716 ± 7.15306
EC	4.03590 ± 0.50550	13.88116 ± 1.24390	15.00094 ± 3.00011	2.44201 ± 0.16082
TC	48.81160 ± 6.64178	48.96327 ± 4.77025	51.41909 ± 4.70279	49.72917 ± 7.31388
OC/EC	11.09	2.53	2.43	19.36
SUM%	64.72789 ± 6.74281	61.14495 ± 4.44584	59.07735 ± 4.31476	58.72564 ± 5.70685

[a] See Table 1 for source profile description.

Table 3
Composite PM$_{10-2.5}$ source profiles (weight percent by mass) of emissions from industrial combustion.

Species	Source type[a]						
	CPI	FEMNI	SPI	CTPP	SRM	EAW	BKP
Al	5.49470 ± 0.33866	4.81750 ± 1.03634	1.35160 ± 0.63216	15.17650 ± 5.11546	0.21030 ± 0.05824	3.02660 ± 0.55120	2.3153 ± 0.46817
As	0.00008 ± 0.00009	0.00297 ± 0.00178	0.00096 ± 0.00061	0.00513 ± 0.00080	0.00135 ± 0.00153	0.05698 ± 0.00622	0.07027 ± 0.01185
Ca	28.3963 ± 3.05191	13.64770 ± 2.64674	2.30300 ± 0.60274	8.28640 ± 0.12662	13.36910 ± 2.30905	1.62330 ± 1.09518	6.6947 ± 3.43744
Cd	0.00002 ± 0.00003	0.00007 ± 0.00041	0.00019 ± 0.00016	0.00003 ± 0.00012	0.00097 ± 0.00072	0.01155 ± 0.00416	0.02892 ± 0.00458
Co	0.00053 ± 0.00021	0.00097 ± 0.00073	0.00011 ± 0.00009	0.00129 ± 0.00048	0.00010 ± 0.00008	0.00105 ± 0.00076	0.00739 ± 0.00284
Cr	0.00094 ± 0.00030	0.02233 ± 0.00288	0.10160 ± 0.01837	0.01403 ± 0.00230	0.01074 ± 0.00081	0.03559 ± 0.00270	0.00809 ± 0.00145
Cu	0.56994 ± 0.03840	0.36238 ± 0.08120	0.07920 ± 0.00843	0.03804 ± 0.02990	0.00535 ± 0.00384	0.08504 ± 0.00623	0.07444 ± 0.00840
Fe	5.0071 ± 0.90288	13.77450 ± 0.56724	21.11040 ± 1.02485	8.41470 ± 0.71907	9.49370 ± 1.07447	32.33830 ± 2.42850	2.9030 ± 0.39124
Hg	0.00066 ± 0.00050	0.00230 ± 0.00267	0.00123 ± 0.00046	0.00120 ± 0.00189	0.00430 ± 0.00318	0.05339 ± 0.00632	0.00593 ± 0.00282
K	0.48897 ± 0.10689	0.47218 ± 0.59938	0.97613 ± 0.71213	0.34940 ± 0.20205	0.49092 ± 0.21016	3.27773 ± 0.33733	0.13954 ± 0.09471
Mg	7.3784 ± 1.28531	3.74070 ± 0.88320	2.19140 ± 1.00629	2.38780 ± 0.50880	2.04370 ± 0.42698	3.96190 ± 0.53262	0.78990 ± 0.11807
Mn	0.05064 ± 0.02885	1.66547 ± 0.12385	0.18754 ± 0.04066	0.22372 ± 0.02576	0.04648 ± 0.01533	3.51595 ± 0.24869	0.00734 ± 0.00084
Mo	0.00073 ± 0.00002	0.00002 ± 0.00002	0.00008 ± 0.00007	0.00001 ± 0.00001	0.00030 ± 0.00022	0.00334 ± 0.00196	0.01954 ± 0.00838
Na	4.8987 ± 0.48663	5.18470 ± 1.26335	1.28560 ± 0.45459	1.34000 ± 0.42339	4.02070 ± 0.42635	2.56630 ± 0.39926	1.65060 ± 0.24713
Ni	0.00156 ± 0.00214	0.01435 ± 0.00884	0.01315 ± 0.00288	0.01578 ± 0.00304	0.00408 ± 0.00393	0.00580 ± 0.00568	0.02504 ± 0.01872
Pb	0.00245 ± 0.00125	0.00051 ± 0.00032	0.00016 ± 0.00006	0.02351 ± 0.00255	1.86596 ± 0.13283	0.37678 ± 0.03016	0.02605 ± 0.00633
S	0.01298 ± 0.00100	0.00841 ± 0.25070	0.00488 ± 0.48098	0.20994 ± 0.03220	0.07954 ± 0.29517	0.00182 ± 0.00526	0.04841 ± 0.00836
Sb	0.00018 ± 0.00014	0.00012 ± 0.00007	0.00003 ± 0.00002	0.00002 ± 0.00002	0.00099 ± 0.00071	0.00379 ± 0.00272	0.02304 ± 0.01065
Se	0.00002 ± 0.00001	0.00014 ± 0.00009	0.00008 ± 0.00008	0.00009 ± 0.00002	0.00091 ± 0.00066	0.00762 ± 0.00275	0.01833 ± 0.00908
V	0.00013 ± 0.00002	0.00478 ± 0.00248	0.00696 ± 0.00661	0.00005 ± 0.00002	0.00560 ± 0.00138	0.00646 ± 0.00169	0.06022 ± 0.02743
Zn	0.03896 ± 0.01686	0.09116 ± 0.13819	0.09714 ± 0.02600	0.09500 ± 0.02990	0.68181 ± 0.14016	0.73546 ± 0.05210	0.07522 ± 0.01364
F$^-$	0.03852 ± 0.04048	0.06715 ± 0.09750	0.01427 ± 0.00304	0.09743 ± 0.08561	0.00693 ± 0.00106	0.33296 ± 0.12073	0.03296 ± 0.00651
Cl$^-$	0.00772 ± 0.00614	0.28784 ± 0.33157	0.31286 ± 0.10486	0.07372 ± 0.04311	0.14006 ± 0.01269	0.14739 ± 0.04329	0.56544 ± 0.17641
NO$_3^-$	0.00172 ± 0.00184	0.21263 ± 0.13472	0.06384 ± 0.05136	0.22759 ± 0.14444	0.28107 ± 0.02674	0.00829 ± 0.00596	0.63741 ± 0.07688
SO$_4^{2-}$	0.63364 ± 0.48367	0.50526 ± 0.28913	0.02006 ± 0.00520	0.50961 ± 0.14754	1.67202 ± 0.68251	0.39700 ± 0.14124	0.18001 ± 0.09616
Na$^+$	1.14263 ± 0.41523	2.03079 ± 0.13616	0.79040 ± 0.25865	0.86871 ± 0.07730	0.72517 ± 0.03961	1.00457 ± 0.06740	0.87461 ± 0.29991
NH$_4^+$	0.00384 ± 0.00087	0.35951 ± 0.06442	0.01989 ± 0.01782	0.19069 ± 0.11778	0.08679 ± 0.00925	0.17020 ± 0.03499	0.37590 ± 0.13970
K$^+$	0.00711 ± 0.00660	0.15456 ± 0.06690	0.02483 ± 0.00660	0.22128 ± 0.02431	0.00797 ± 0.01225	3.14997 ± 0.24017	0.11668 ± 0.02232
Ca^{2+}	5.61426 ± 1.01488	1.41889 ± 0.17508	1.14944 ± 1.03219	1.62167 ± 0.57040	2.47649 ± 0.45340	0.87500 ± 0.11248	1.76475 ± 0.21570
Mg^{2+}	0.13597 ± 0.11344	0.78699 ± 0.25645	0.65474 ± 0.51390	0.69435 ± 0.24237	0.37625 ± 0.08420	0.36965 ± 0.09224	0.25984 ± 0.05840
OC	2.2486 ± 2.32368	2.87288 ± 1.22745	2.27037 ± 1.85398	8.84522 ± 1.35123	8.09539 ± 2.10477	0.30957 ± 0.07548	13.97630 ± 0.69881
EC	0.07027 ± 0.03100	3.79361 ± 1.67288	8.18403 ± 2.61525	4.03326 ± 0.58790	2.07284 ± 0.10364	0.02096 ± 0.00310	24.35658 ± 1.31783
TC	2.31887 ± 2.35468	6.66649 ± 2.90033	10.4544 ± 4.46923	12.87848 ± 1.93913	10.16823 ± 2.20841	0.33053 ± 0.07858	38.33288 ± 2.01664
OC/EC	31.99	0.76	0.28	2.19	3.91	14.77	0.57
SUM%	55.34829 ± 5.15047	51.91213 ± 4.42815	40.59677 ± 3.66975	50.56015 ± 3.70200	44.69199 ± 2.64570	53.08110 ± 5.14628	55.14317 ± 4.40443

[a] See Table 1 for source profile description.

K$^+$ (2.69 ± 0.371%) in RSFS is 15 to 21-fold higher than abundances for RKS and RLPGS; whereas the abundance of NH$_4^+$ (1.9 ± 0.26%) in RKS is 2 to 38-fold higher than those for RSFS and RLPGS, similar to past studies for kerosene stoves (Matawle et al., 2014; Patil et al., 2013). The abundance of sulfur constituents (S and SO$_4^{2-}$) along with Cd, Hg, Ni, Pb, V and Zn are higher for RKS than for RSFS and RLPGS. Abundances of several anions (NO$_3^-$, F$^-$ and Cl$^-$) in RSFS are also higher than those for RKS and RLPGS.

3.4. Mineral-based coal-fired industries

Six major mineral-based coal-fired industrial emissions were sampled. The highest EC abundance (24 ± 1.3%) was found for the brick kiln (BKP) with an OC/EC ratio of 0.57. The iron (Fe) abundance (21.1 ± 1%) for steel production (SPI) was 1.53–7.20 fold higher than that for other industrial processes, whereas the abundances of Al (15.2 ± 5.1%) and Ca (28.4 ± 3.1%) were elevated for cement production. The highest K$^+$/K ratio (0.84) was found for BKP, different from those reported for coal-fired industries (CPCB, 2008; USEPA, 2013; Watson et al., 2001). This might be due to the use of dung cakes with coal in brick kilns. Owing to the similar origins of the coal (Volkovic, 1983), sulfur (S, 0.002–0.2%), sulfate (SO$_4^{2-}$, 0.02–1.7%), and selenium (Se, 0.00002–0.018%) abundances were similar for all.

Large variations were found in trace element abundances. The highest abundances of toxic species (As, Cd, Co, Mo, Sb and V) were measured for the BKP, followed by Hg in steel rolling mills (SRM) and Ni in steel production (SPI). Toxic species are emitted mostly from incomplete combustion of biofuels (coal, wood, dung cakes etc.) at moderate combustion temperatures (Vollkovic, 1983). Supplemental Table

S2 compared CTPP profile with past studies (Bi et al., 2007; Chow et al., 2004; CPCB, 2008a; Yatkin and Bayram, 2008).

3.5. Electric arc-welding

Open fabrication workshop emissions with electric arc-welding activities (EAW) (Pervez et al., 2005) were dominated by Fe (32.3 ± 2.4%), K (3.3 ± 0.33%), and Mn (3.5 ± 0.25%). Abundances of As, Cu, Zn, and F$^-$ were in the range of 0.3–0.7%, higher than those reported (<0.1%) in other studies (CPCB, 2008; Matawle et al., 2014; Swamy et al., 1994).

4. Discussion

Similarities and differences of measured source profiles were evaluated using mass reconstruction, coefficient of divergence (co-linearity between source profiles), and enrichment factors.

4.1. Mass reconstruction

Mass reconstruction has been used to account for the unmeasured oxygen (O) and hydrogen (H) and to achieve closure between gravimetric mass and the sum of measured species concentrations (Watson et al., 2012; Chow et al., 2015). Fig. 1 displays the mass reconstruction in seven categories (Geological material, other elements, sulphate, other ions, OM, and EC) (Chow et al., 2015; Pei et al., 2016). Excellent mass reconstruction was achieved for residual solid fuel combustion (RSFS, 100.56%), electric-arc welding (EAW, 98.6%), and municipal solid waste combustion (MSWB, 97.1%). Low mass reconstructions
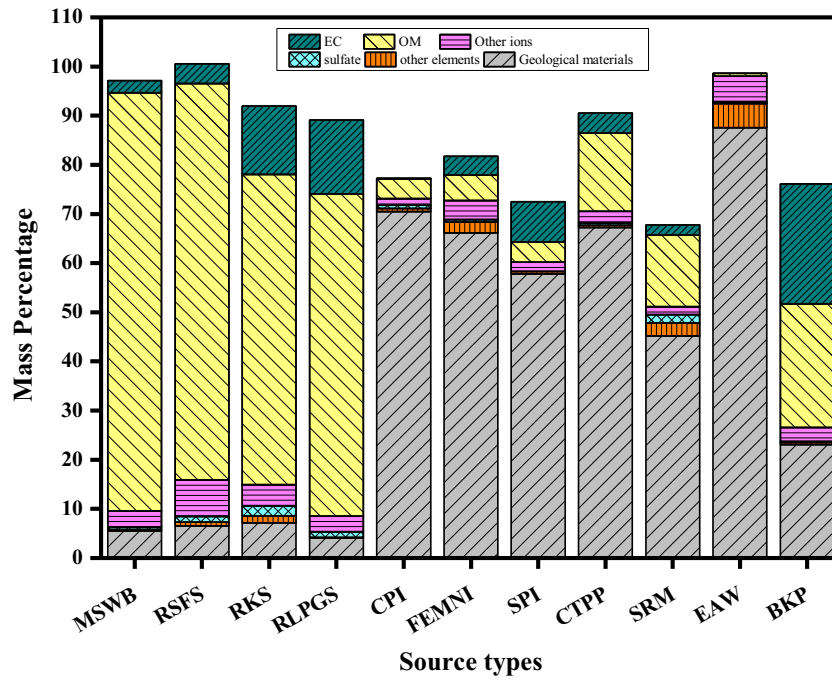
Fig. 1. $PM_{10-2.5}$ mass reconstruction for domestic cooking and industrial combustion sources (See Table 1 for source type description). Geological material = $2.2 \times Al + 1.63 \times Ca + 2.42 \times Fe$; Other elements are the sum of all measured elements excluding Na, Mg, Al, S, K, Ca, and Fe; other ions are the sum of 9 measured ions excluding SO_4^{2-} and Ca^{2+}; and OM = $1.8 \times OC$.

were found for steel rolling mills (SRM, 67.8%), steel production (SPI, 72.5%), and cement production (CPI, 77.3%). Industrial sources exhibited high geological components (30–91%), whereas municipal solid waste and household fuel combustion sources showed abundant organic matter (OM, 69–88%), comparable to those reported by Matawle et al. (2014).

4.2. Coefficients of divergence (COD)

The coefficients of divergence (COD) is used to evaluate the similarities and differences among the profiles. COD is a self-normalizing parameter which measures the spread of the data (Kong et al., 2011, 2014; Matawle et al., 2015). The COD was calculated using the following formula (Feng et al., 2007; Han et al., 2010; Wongphatarakul et al., 1998; Zhang and Friedlander, 2000):

$$CODjk = \sqrt{\frac{1}{p}\sum_{i=1}^{p}\left(\frac{X_{ij}-X_{ik}}{X_{ij}+X_{ik}}\right)^2} \qquad (1)$$

where j and k refer to the two profiles; p is the number of investigated components; X_{ij} and X_{ik} represent the average mass concentrations of

chemical component i for profiles j and k. The two sources are similar if COD approaches zero; if COD_{jk} values approaches one, the two sources are considered different. A COD value ≤0.269 represents similarities between profiles (Wongphatarakul et al., 1998). Table 4 showed high COD values (0.46–0.88), indicating that the profiles are different. The lowest COD value (0.46) is found between coal-based thermal plant (CTPP) and ferro-manganese (FEMNI) profiles, whereas the highest COD value is found between the cement production (CPI) and the residential kerosene stove (RKS) profiles.

4.3. Enrichment factors (EFs)

Enrichment factors (EFs) are normalized elemental concentrations as a ratio to another constituent present in all of the profiles. There is no consensus about the most appropriate element to be used for normalization. This study selected two of the most abundant elements: calcium (Ca) for cement production (CPI) and iron (Fe) for steel production (SPI) and coal-based power plant (CTPP), using the raw material as an elemental reference to examine the effect of high-temperature industrial process on enrichments (Volkovic, 1983; Sharma and Pervez, 2004a). EFs relative to a base material (Cao et al., 2008) were

Table 4
Coefficients of divergence (COD) for $PM_{10-2.5}$ combustion sources.

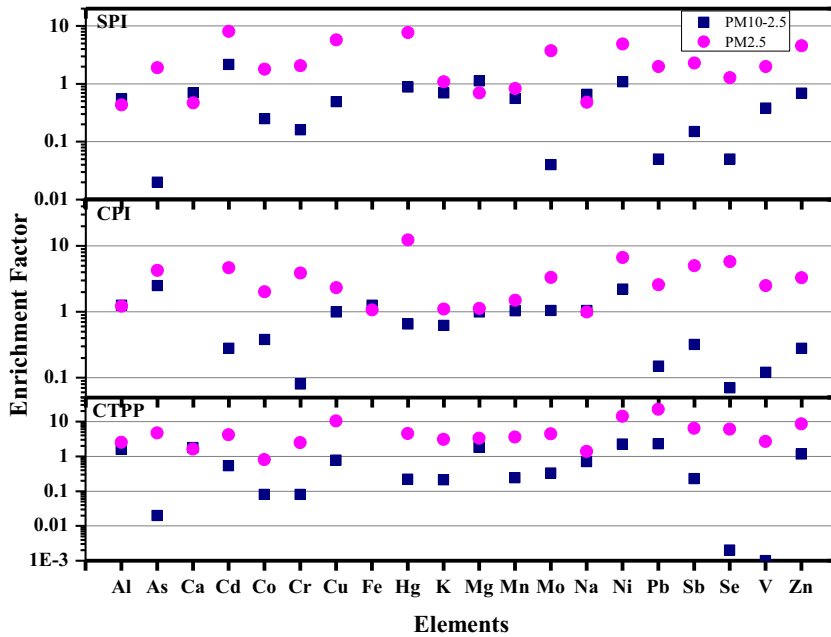|	MSWB	RSFS	RKS	RLPGS	CPI	FEMNI	SPI	CTPP	SRM	BKP	EAW
MSWB	0.00										
RSFS	0.55	0.00									
RKS	0.71	0.76	0.00								
RLPGS	0.64	0.74	0.60	0.00							
CPI	0.72	0.75	0.88	0.79	0.00						
FEMNI	0.61	0.69	0.77	0.70	0.64	0.00					
SPI	0.64	0.69	0.81	0.74	0.70	0.51	0.00				
CTPP	0.67	0.66	0.79	0.76	0.67	0.46	0.59	0.00			
SRM	0.62	0.67	0.72	0.69	0.70	0.61	0.61	0.62	0.00		
BKP	0.63	0.65	0.75	0.71	0.75	0.64	0.69	0.60	0.67	0.00	
EAW	0.66	0.72	0.78	0.77	0.77	0.66	0.70	0.71	0.70	0.68	0.00

Fig. 2. Enrichment factors of inorganic species in $PM_{10-2.5}$ and $PM_{2.5}$ emissions from selected coal-fired metallurgical Industries.

calculated using the following formula:

$$EF = \frac{(Concentration\ of\ element / Concentration\ of\ Reference)_{sample}}{(Concentration\ of\ element / Concentration\ of\ Reference)_{base\ material}} \quad (2)$$

For bituminous coal, raw material collected from a 500 MW thermal power plant in Purena, Bhilai is used as base material. Steel process industries have reported ~58.3% iron ore, 29.15% coke, 6.99% limestone, 4.66% dolomite, 0.58% ferro-manganese, and 0.29% ferrosilicon (Quraishi, 1997; Sharma, 2002) - a similar composition was used as base material. Cement production consists of ~75% calcium carbonate ($CaCO_3$), 20% of silica (SiO_2), alumina (Al_2O_3), and iron oxide (Fe_2O_3), and the remaining 5% of magnesium carbonate, sulfur, and alkalis (Eckel and Bain, 1905) - a similar composition was used as base

material. Comparisons of EFs between $PM_{10-2.5}$ and previous published $PM_{2.5}$ profiles (Matawle et al., 2014) are presented in Fig. 2 and Supplemental Table S3. EFs for $PM_{10-2.5}$ elemental species in selected source emissions are also compared in Fig. 3.

For $PM_{10-2.5}$ (Table S3), the highest EF values were obtained for Cd (2.16) in SPI, As (2.49) in CPI and Pb (2.31) in CTPP with low As (0.02), Se (0.002–0.07) and V (0.001–0.38), consistent with past studies (Bhangare et al., 2011; Kong et al., 2011; Sharma and Pervez, 2004b). For $PM_{2.5}$, the highest EF values were obtained for Hg (12.34) in CPI, Cd (8.10) for SPI and Pb (22.63) for CTPP. Overall, CTPP has the highest EFs for Al, Ca, Mg, Ni, Pb, Zn; SPI has the highest EFs for Cd, Hg, V, Se; and CPI has the highest EFs for As, Co, Cu, Fe, Mn, Mo, Na, Sb in $PM_{10-2.5}$. Fig. 2 depicts agreement with earlier findings (Volkovic, 1983) that higher combustion temperatures (950–1200 °C) result in higher enrichment
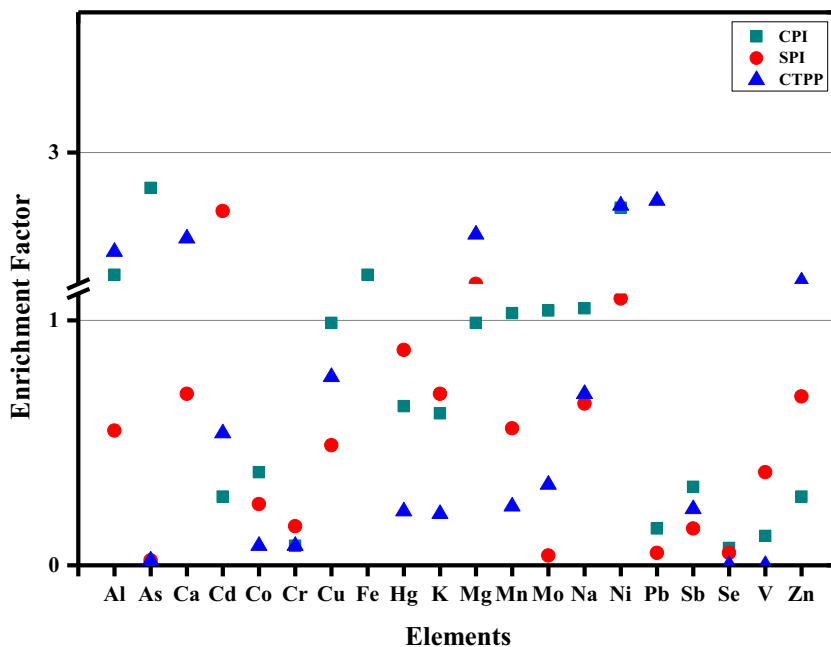

Fig. 3. Comparison of elemental enrichment factors in $PM_{10-2.5}$ emissions from selected coal-fired metallurgical industries.

Table 5
Source markers in PM$_{10-2.5}$ combustion sources.

Aerosol fractions	Source signatures	References
Domestic heating activities		
1. Residential solid fuel burning (RSFS)		
PM$_{10-2.5}$	*As, Cr, K, NO$_3^-$, K$^+$, and EC*	Present study
PM$_{2.5}$	*F$^-$, As, Mg^{2+}, Ca^{2+}, Cr, and K$^+$*	Matawle et al., 2014
PM$_{2.5}$	*K, EC, OC, and Br*	Guttikunda, 2009
PM$_{2.5}$	*OC, EC, K+, and Cl-*	Watson et al., 2008
2. Residential kerosene stoves (RKS)		
PM$_{10-2.5}$	*K, Pb, V, NH$_4^+$, K$^+$, and EC*	Present study
PM$_{2.5}$	*Pb, Cd, Sb, F–, Se, and V*	Matawle et al., 2014
3. Residential LPG stoves (RLPGS)		
PM$_{10-2.5}$	*Mo, Pb, Se, K$^+$, OC, and EC*	Present study
PM$_{2.5}$	*Sb, Cd, Pb, S, Mo, and Se*	Matawle et al., 2014
4. Municipal solid waste burning (MSWB)		
PM$_{10-2.5}$	*Cd, K, Mo, NO$_3^-$, K$^+$, and OC*	Present study
PM$_{2.5}$	*F$^-$, Co, Cd, Ca^{2+}, Na$^+$, and K$^+$*	Matawle et al., 2014
PM	*K, Zn, Pb, and Sb*	Guttikunda, 2009
PM$_{2.5}$	*OC, EC, K$^+$, As, Pb, and Zn*	Watson et al., 2008
PM	*Zn, Sb, Cu, Cd, and Hg*	Mitra et al., 2002
Industrial sources		
5. Cement production industry (CPI)		
PM$_{10-2.5}$	*Al, Ca, Cu, Mg, Ca^{2+}, and Mg^{2+}*	Present study
PM$_{2.5}$	*S, Cr, Cu, Al, Mo, and Mg*	Matawle et al., 2014
PM$_{10}$	*Zn, S, Mg^{2+}, SO$_4^{2-}$, Ca, and Mg, and*	Kong et al., 2011
PM	*Ca*	Guttikunda, 2009
6. Ferro-manganese industry (FEMNI)		
PM$_{10-2.5}$	*Cu, Fe, Mg, Mn, NO$_3^-$, and Mg^{2+}*	Present study
PM$_{2.5}$	*Cr, Mo, Mg^{2+}, Mn, NO$_3^-$, and Cu*	Matawle et al., 2014
7. Steel production industry (SPI)		
PM$_{10-2.5}$	*Al, Cr, Fe, Mg, and Mg^{2+}+EC*	Present study
PM$_{2.5}$	*Cr, As, Mg^{2+}, Cu, EC, and Cl$^-$*	Matawle et al., 2014
PM	*Mn, Cr, Fe, Zn, W, Rb*	Guttikunda, 2009
PM$_{10}$	*V, Ni, and SO$_4^{2-}$*	Viana et al., 2008
PM$_{2.5}$	*Zn, Pb, Cu, Mn, As, and Hg*	Watson et al., 2008
8. Coal based thermal power plant (CTPP)		
PM$_{10-2.5}$	*As, S, F-, NO$_3^-$ K+, and Mg^{2+}*	Present study
PM$_{2.5}$	*As, Cr, S, F–, NO$_3^-$, and Al*	Matawle et al., 2014
PM$_{10}$	*Zn, NO$_3^-$, Mg^{2+}, Cl$^-$, S, and Ni*	Kong et al., 2011
PM	*Al, Sc, Se, Co, As, Ti, Th, and S*	Guttikunda, 2009
PM	*Se, As, Cr, Co, Cu, and Al*	Mitra et al., 2002
9. Steel rolling mills (SRM)		
PM$_{10-2.5}$	*Fe, Mg, Pb, NO$_3^-$, SO$_4^{2-}$, and Mg^{2+}*	Present study
PM$_{2.5}$	*Pb, Mg^{2+}, NO$_3^-$, EC, S, and Cl*	Matawle et al., 2014
10. Fabrication and welding (EAW)		
PM$_{10-2.5}$	*Cd, K, Mg, Mn, Pb, and K+*	Present study
PM$_{2.5}$	*Mn, Cr, K+, Cd, Pb, and Mg^2+*	Matawle et al., 2014
PM$_{2.5}$	*SO$_4^{2-}$, Se, V, Ni, OC, and EC*	Watson et al., 2008

Table 5 (continued)

Aerosol fractions	Source signatures	References
11. Brick kiln process (BKP)		
PM$_{10-2.5}$	*As, Cd, Pb, Sb, NO$_3^-$, and EC*	Present study
PM$_{2.5}$	*As, Cd, Mo, EC, NO$_3^-$, and Sb*	Matawle et al., 2014

of the toxic metals. Elements like Al, Ca, Fe, Na, and K have similar EFs, for both PM$_{10-2.5}$ and PM$_{2.5}$. In contrast, Se, V, Sb have the largest differences between PM$_{10-2.5}$ and PM$_{2.5}$.

4.4. Source markers

Source markers have been evaluated by using the following formula (Kong et al., 2011; Yang et al., 2002):

$$Ratio\, j, i = \frac{(X_i/\sum X)_j}{(X_i/\sum X)_{min}} \qquad (3)$$

where X_i is the ith individual species concentration; $(X_i/\Sigma X)_j$ is the abundance of the ith individual species divided by the sum of 32 species concentrations for source j; $(X_i/\Sigma X)_{min}$ is the minimum abundance of the ith individual species divided by the sum of 32 species concentrations (Chen et al., 2003; Yang et al., 2002). To minimize the effects of physical parameters, a normalization procedure was applied (Mitra et al., 2002; Kong et al., 2011). Normalized individual species concentrations were divided by the ith individual species concentration to the sum of ith individual concentration for all the source profiles (Kong et al., 2011). The top six chemical species with the highest values for these ratios are the representative source markers. Findings and comparison with reported values (Mitra et al., 2002; Viana et al., 2008; Watson et al., 2008; Guttikunda, 2009; Kong et al., 2011; Matawle et al., 2014) are presented in Table 5.

Water-soluble K$^+$ is a marker for biomass burning sources (Watson et al., 2002, 2008). Table 5 shows that both K$^+$ and NO$_3^-$ can be used as markers for MSWB and RSFS whereas EC is a source marker for all three-household fuel combustion sources (RSFS, RKS and RLPGS). Mn is a marker for FEMNI and EAW, whereas Fe can be a marker for FEMNI, SPI, and SRM. As is a marker for coal burning (Mitra et al., 2002), with a similar result found for CTPP and BKP; consistent with those reported in Matawle et al. (2014). Emissions from domestic cooking activities show a higher degree of dissimilarity than the industrial source types. Diversity in the observed source markers (Mitra et al., 2002; Viana et al., 2008; Watson et al., 2008; Matawle et al., 2014) suggests the importance in developing region-specific source profiles to obtaining accurate source apportionment results.

5. Conclusions

Chemical source profiles for coarse (PM$_{10-2.5}$ µm) particles for eleven domestic cooking and industrial sources have been documented. Carbon (OC + EC) is the most abundant fraction in household cooking and municipal solid waste burning emissions (49–51%) with OC/TC ratios ranging 2.4–19.4, whereas geological materials are most abundant in industrial sources, contributing 26–95% of the total measured mass. Source markers have been identified as K$^+$, OC, and EC for household-fuel combustion while Mn and As are markers for metallurgical industries and coal burning, respectively. PM$_{10-2.5}$ mass reconstructions achieved 89–101% for domestic cooking stoves, 97% for municipal solid waste combustion, and 68–98% for industrial combustion processes. Significant differences among PM$_{10-2.5}$ profiles were found with large coefficients of divergence (CODs) ranging 0.46–0.88. Enrichment factors (EFs) showed elevated Cd (2.16) for steel production, As (2.49) for cement production, and Pb (2.31) for coal-based thermal

power plants. Most of the elements were enriched in $PM_{2.5}$ as compared to $PM_{10–2.5}$. Results from the study can be used for source apportionment as well as for emission inventory calculations.

Acknowledgements

Appendix A. Supplementary data

Supplementary data to this article can be found online at https://doi.org/10.1016/j.scitotenv.2018.01.289.

References

Aldabe, J., Elustondo, D., Santamaría, C., Lasheras, E., Pandolfi, M., Alastuey, A., Querol, X., Santamaría, J.M., 2011. Chemical characterisation and source apportionment of $PM_{2.5}$ and PM_{10} at rural, urban and traffic sites in Navarra (North of Spain). Atmos. Res. 102, 191–205.

Bhangare, R.C., Ajmal, P.Y., Sahu, S.K., Pandit, G.G., Puranik, V.D., 2011. Distribution of trace elements in coal and combustion residues from five thermal power plants in India. Int. J. Coal Geol. 86, 349–356.

Bi, X., Feng, Y., Wu, J., Wang, Y., Zhu, T., 2007. Source apportionment of PM_{10} in six cities of northern China. Atmos. Environ. 41, 903–912.

Cao, J.J., Chow, J.C., Watson, J.G., Wu, F., Han, Y.M., Jin, Z.D., Shen, Z.X., An, Z.S., 2008. Size-differentiated source profiles for fugitive dust in the Chinese Loess Plateau. Atmos. Environ. 42, 2261–2275.

Census, 2011. Office of the Registrar General and Census Commissioner, India. Available from:. http://www.censusindia.gov.in/2011.

Chakrabarty, R.K., Pervez, S., Chow, J.C., Watson, J.G., Dewangan, S., Robles, J., Tian, G., 2013. Funeral pyres in South Asia: brown carbon aerosol emissions and climate impacts. Environ. Sci. Technol. Lett. 1, 44–48.

Chelani, A.B., Gajghate, D.G., Devotta, S., 2008. Source apportionment of PM_{10} in Mumbai, India using CMB model. Bull. Environ. Contam. Toxicol. 81, 190–195.

Chen, S.-J., Hsieh, L.-T., Chiu, S.-C., 2003. Emission of polycyclic aromatic hydrocarbons from animal carcass incinerators. Sci. Total Environ. 313, 61–76.

Chow, J.C., Watson, J.G., 2017. Enhanced ion chromatographic speciation of water-soluble $PM_{2.5}$ to improve aerosol source apportionment. Aerosol Sci. Eng. 1 (1), 7–24.

Chow, J.C., Watson, J.G., Ashbaugh, L.L., Magliano, K.L., 2003. Similarities and differences in PM_{10} chemical source profiles for geological dust from the San Joaquin Valley, California. Atmos. Environ. 37, 1317–1340.

Chow, J.C., Watson, J.G., Kuhns, H., Etyemezian, V., Lowenthal, D.H., Crow, D., Kohl, S.D., Engelbrecht, J.P., Green, M.C., 2004. Source profiles for industrial, mobile, and area sources in the Big Bend Regional Aerosol Visibility and Observational study. Chemosphere 54, 185–208.

Chow, J.C., Lowenthal, D.H., Chen, L.-W.A., Wang, X., Watson, J.G., 2015. Mass reconstruction methods for $PM_{2.5}$: a review. Air Qual. Atmos. Health 8, 243–263.

CPCB, 2008. Stationary sources emission profiles, Central Pollution Control Board, Delhi. Available from. http://www.cpcb.nic.in/Stationary_Sources_Emission_Profiles.xls.

Dewangan, S., Chakrabarty, R., Zielinska, B., Pervez, S., 2013. Emission of volatile organic compounds from religious and ritual activities in India. Environ. Monit. Assess. 185 (11), 9279–9286.

Eckel, E.C., Bain, H.F., 1905. Cement and cement materials of Iowa. Iowa Geol. Surv. Annu. Rep. 15, 33–124.

Feng, Y., Xue, Y., Chen, X., Wu, J., Zhu, T., Bai, Z., Fu, S., Gu, C., 2007. Source apportionment of ambient total suspended particulates and coarse particulate matter in urban areas of Jiaozuo, China. J. Air Waste Manage. Assoc. 57, 561–575.

Friedlander, S.K., 1973. Chemical element balances and identification of air pollution sources. Environ. Sci. Technol. 7 (United States).

Gokhale, S., Kohajda, T., Schlink, U., 2008. Source apportionment of human personal exposure to volatile organic compounds in homes, offices and outdoors by chemical mass balance and genetic algorithm receptor models. Sci. Total Environ. 407, 122–138.

Gupta, A.K., Karar, K., Srivastava, A., 2007. Chemical mass balance source apportionment of PM_{10} and TSP in residential and industrial sites of an urban region of Kolkata, India. J. Hazard. Mater. 142, 279–287.

Guttikunda, S.K., 2009. Urban particulate pollution source apportionment: part 1—definition, methodology, and resources. Simple Interact. Model. Better Air Qual. SIM-air Work. Pap. Ser 16.

Han, B., Kong, S., Bai, Z., Du, G., Bi, T., Li, X., Shi, G., Hu, Y., 2010. Characterization of elemental species in $PM_{2.5}$ samples collected in four cities of Northeast China. Water Air Soil Pollut. 209, 15–28.

Ho, K.F., Lee, S.C., Chow, J.C., Watson, J.G., 2003. Characterization of PM_{10} and $PM_{2.5}$ source profiles for fugitive dust in Hong Kong. Atmos. Environ. 37, 1023–1032.

Kong, S., Ji, Y., Lu, B., Chen, L., Han, B., Li, Z., Bai, Z., 2011. Characterization of PM_{10} source profiles for fugitive dust in Fushun-a city famous for coal. Atmos. Environ. 45, 5351–5365.

Kong, S., Ji, Y., Lu, B., Zhao, X., Han, B., Bai, Z., 2014. Similarities and differences in $PM_{2.5}$, PM_{10} and TSP chemical profiles of fugitive dust sources in a coastal oilfield city in China. Aerosol Air Qual. Res. 14, 2017–2028.

Liu, Y., Zhang, W., Bai, Z., Yang, W., Zhao, X., Han, B., Wang, X., 2017. China source profile shared service (CSPSS): the Chinese $PM_{2.5}$ database for source profiles. Aerosol Air Qual. Res. 17, 1401–1414.

Matawle, J., Pervez, S., Dewangan, S., Tiwari, S., Bisht, D.S., Pervez, Y.F., 2014. $PM_{2.5}$ chemical source profiles of emissions resulting from industrial and domestic burning activities in India. Aerosol Air Qual. Res. 14, 2051–2066.

Matawle, J.L., Pervez, S., Dewangan, S., Shrivastava, A., Tiwari, S., Pant, P., Deb, M.K., Pervez, Y., 2015. Characterization of $PM_{2.5}$ source profiles for traffic and dust sources in Raipur, India. Aerosol Air Qual. Res. 15, 2537–2548.

Mitra, A.P., Morawska, L., Sharma, C., Zhang, J., 2002. Chapter two: methodologies for characterisation of combustion sources and for quantification of their emissions. Chemosphere 49, 903–922.

Ning, D.-T., Zhong, L.-X., Chung, Y.-S., 1996. Aerosol size distribution and elemental composition in urban areas of northern China. Atmos. Environ. 30, 2355–2362.

Patil, R.S., Kumar, R., Menon, R., Shah, M.K., Sethi, V., 2013. Development of particulate matter speciation profiles for major sources in six cities in India. Atmos. Res. 132, 1–11.

Pei, B., Wang, X., Zhang, Y., Hu, M., Sun, Y., Deng, J., Dong, L., Fu, Q., Yan, N., 2016. Emissions and source profiles of $PM_{2.5}$ for coal-fired boilers in the Shanghai megacity, China. Atmos. Pollut. Res. 7, 577–584.

Pernigotti, D., Belis, C.A., Spanò, L., 2016. SPECIEUROPE: the European data base for PM source profiles. Atmos. Pollut. Res. 7, 307–314.

Pervez, S., Mathew, J., Sharma, R., 2005. Investigation of personal-indoor-outdoor particulate relationships in welding workshops. J. Sci. Ind. Res. (CSIR, India) 64, 454–458.

Quraishi, Y.F., 1997. Study of Physico-chemical Characteristics of Fugitive Dusts in Relation to Respiratory Ailments. (Ph. D. Thesis). Pt. Ravishankar Shukla University, Raipur, India.

Rumana, H.S., Sharma, R.C., Beniwal, V., Sharma, A.K., 2014. A retrospective approach to assess human health risks associated with growing air pollution in urbanized area of Thar desert, Western Rajasthan, India. J. Environ. Health Sci. Eng. https://doi.org/10.1186/2052-336X-12-23.

Samara, C., Kouimtzis, T., Tsitouridou, R., Kanias, G., Simeonov, V., 2003. Chemical mass balance source apportionment of PM_{10} in an industrialized urban area of Northern Greece. Atmos. Environ. 37, 41–54.

Samiksha, S., Raman, R.S., Nirmalkar, J., Kumar, S., Sirvaiya, R., 2017. PM_{10} and $PM_{2.5}$ chemical source profiles with optical attenuation and health risk indicators of paved and unpaved road dust in Bhopal, India. Environ. Pollut. 222, 477–485.

Sharma, R., 2002. Characterization and Impact Assessment of Emitted Dusts in Selected Environments. (Ph. D. Thesis). Pt. Ravishankar Shukla University, Raipur, India.

Sharma, R., Pervez, S., 2004a. A case study of spatial variation and enrichment of selected elements in ambient particulate matter around a large coal-fired power station in central India. Environ. Geochem. Health 26:373–381. https://doi.org/10.1007/s10653-005-6369-1.

Sharma, R., Pervez, S., 2004b. Chemical Characterization and Enrichment of Selected Toxic Elements in Ambient Particulate Matter around a Slag Based Cement Plant in Chhattisgarh State-A Case Study.

Srivastava, A., Gupta, S., Jain, V.K., 2009. Winter-time size distribution and source apportionment of total suspended particulate matter and associated metals in Delhi. Atmos. Res. 92, 88–99.

Swamy, K., Kaliaperumal, R., Swaminathan, G.S., 1994. Wavelength-dispersive X-ray fluorescence spectrometric technique for determining elements in weld fumes. X-Ray Spectrom. 23, 71–74.

Tiwari, S., Pervez, S., Perrino, C., Srivastava, A.K., Bisht, D.S., Chate, D.M., 2013. Chemical characterization of atmospheric particulate matter in Delhi, India, part II: source apportionment studies using PMF 3.0. Sustain. Environ. Res. 23 (5), 295–306.

Tsai, J.-H., Lin, K.-H., Chen, C.-Y., Ding, J.-Y., Choa, C.-G., Chiang, H.-L., 2007. Chemical constituents in particulate emissions from an integrated iron and steel facility. J. Hazard. Mater. 147, 111–119.

USEPA, 2013. PM composite profiles by source category. Available from:. http://cfpub.epa.gov/si/speciate/ehpa_speciate_browse.cfm.

Viana, M., Kuhlbusch, T.A.J., Querol, X., Alastuey, A., Harrison, R.M., Hopke, P.K., Winiwarter, W., Vallius, M., Szidat, S., Prévôt, A.S.H., 2008. Source apportionment of particulate matter in Europe: a review of methods and results. J. Aerosol Sci. 39, 827–849.

Volkovic, V., 1983. Trace Elements in Coal. Vol. II. CRC Press, Florida.

Watson, J.G., Chow, J.C., 2001. Source characterization of major emission sources in the Imperial and Mexicali Valleys along the US/Mexico border. Sci. Total Environ. 276, 33–47.

Watson, J.G., Chow, J.C., Lu, Z., Fujita, E.M., Lowenthal, D.H., Lawson, D.R., Ashbaugh, L.L., 1994. Chemical mass balance source apportionment of PM_{10} during the Southern California Air Quality Study. Aerosol Sci. Technol. 21, 1–36.

Watson, J.G., Chow, J.C., Houck, J.E., 2001. $PM_{2.5}$ chemical source profiles for vehicle exhaust, vegetative burning, geological material, and coal burning in Northwestern Colorado during 1995. Chemosphere 43, 1141–1151.

Watson, J.G., Zhu, T., Chow, J.C., Engelbrecht, J., Fujita, E.M., Wilson, W.E., 2002. Receptor modeling application framework for particle source apportionment. Chemosphere 49, 1093–1136.

Watson, J.G., Antony Chen, L.-W., Chow, J.C., Doraiswamy, P., Lowenthal, D.H., 2008. Source apportionment: findings from the US supersites program. J. Air Waste Manage. Assoc. 58, 265–288.

Watson, J.G., Chow, J.C., Lowenthal, D.H., Chen, L.-W.A., Wang, X., Biscay, P., 2012. Reformulation of PM$_{2.5}$ Mass Reconstruction Assumptions for the San Joaquin Valley Final Report.

Watson, J.G., Chow, J.C., Chen, L.W.A., Engling, G., Wang, X.L., 2016. Source apportionment: principles and methods. Airborne Particulate Matter. Royal Society of Chemistry, pp. 72–125.

Watson, J.G., Tropp, R.J., Kohl, S.D., Wang, X., Chow, J.C., 2017. Filter processing and gravimetric analysis for suspended particulate matter samples. Aerosol Sci. Eng. 1 (2), 93–105.

WHO, 2014. Burden of Disease From the Joint Effects of Household and Ambient Air Pollution for 2012. World Health Organization, Geneva http://www.who.int/phe/health_topics/outdoorair/databases/FINAL_HAP_AAP_BoD_24March2014.pdf?ua=1.

Wongphatarakul, V., Friedlander, S.K., Pinto, J.P., 1998. A comparative study of PM$_{2.5}$ ambient aerosol chemical databases. Environ. Sci. Technol. 32, 3926–3934.

Yang, H.-H., Lai, S.-O., Hsieh, L.-T., Hsueh, H.-J., Chi, T.-W., 2002. Profiles of PAH emission from steel and iron industries. Chemosphere 48, 1061–1074.

Yatkin, S., Bayram, A., 2008. Determination of major natural and anthropogenic source profiles for particulate matter and trace elements in Izmir, Turkey. Chemosphere 71, 685–696.

Zhang, Z., Friedlander, S.K., 2000. A comparative study of chemical databases for fine particle Chinese aerosols. Environ. Sci. Technol. 34, 4687–4694.